

Stacked white organic light emitting devices consisting of separate red, green, and blue elements

Xiangfei Qi,¹ Michael Slightsky,¹ and Stephen Forrest^{2,a)}

¹Department of Physics, University of Michigan, Ann Arbor, Michigan 48109, USA

²Departments of Electrical Engineering and Computer Science, Physics, and Materials Science and Engineering, University of Michigan, Ann Arbor, Michigan 48109, USA

(Received 11 October 2008; accepted 18 October 2008; published online 13 November 2008)

We demonstrate a white organic light-emitting device where individual red, green, and blue (R, G, and B) phosphorescent organic light-emitting devices are vertically stacked and electrically interconnected by a compound MoO₃/Li-doped charge generation layer. For the order of B, G, and R cells positioned relative to the indium tin oxide anode, the device yields a peak total external quantum efficiency (EQE) and power efficiency (PE) of $\eta_{\text{ext}}=(36\pm 2)\%$ at a current density of $J=82\ \mu\text{A}/\text{cm}^2$ and $\eta_p=21\pm 1\ \text{lm}/\text{W}$ at $J=17\ \mu\text{A}/\text{cm}^2$, respectively. The EQE and PE of the device roll off to $(32\pm 2)\%$ and $13\pm 1\ \text{lm}/\text{W}$ at $1000\ \text{cd}/\text{m}^2$, corresponding to $J=2\ \text{mA}/\text{cm}^2$. At this luminance, the device shows Commission Internationale de L'Eclairage chromaticity coordinates of (0.45, 0.36) and a color rendering index of 63. © 2008 American Institute of Physics. [DOI: 10.1063/1.3021014]

White organic light-emitting devices (WOLEDs) have shown their potential for a new generation of solid-state lighting sources.^{1,2} In these applications, it is essential to obtain high efficiency at high luminance ($>1000\ \text{cd}/\text{m}^2$). Conventional WOLEDs employ red, green, and blue (R, G, and B) phosphorescent and/or fluorescent dopants in either a single emission layer (EML) or multiple doped layers that allow for exciton formation in an expanded region.³⁻⁵ Although the latter structure has shown an external quantum efficiency (EQE) approaching 20% in the forward viewing direction, finding a suitable combination of hosts and phosphorescent dopants can be difficult due to the several constraints that are placed on the relative energies of the constituent materials in these architectures.

To achieve high brightness and efficiency at low current density, increasing attention has been directed toward the stacked OLED, or SOLED, where individual OLED emitting elements are electrically connected in series in a vertical configuration.⁶⁻⁸ The connecting charge generating layers (CGLs) are formed by contact of an *n*-doped electron transporting layer (ETL) with either a *p*-doped hole transporting layer (HTL)^{9,10} or with transparent inorganic conductors.¹¹

In the stacked structure reported here (the RGB SOLED), individual primary-color-emitting phosphorescent OLEDs are interconnected by Li-doped 4,7-diphenyl-1,10-phenanthroline (BPhen) and MoO₃ to form a compound CGL. A recent report used fluorescent emitting regions separated by a CGL to achieve white light.¹² In contrast, our device utilizes all electrophosphorescent R, G, and B elements to achieve high efficiency white luminance. The luminance at a fixed current density is approximately equal to the sum of that for each independent OLED element.

Figure 1(a) shows the schematic energy level diagram of the RGB SOLED consisting of three interconnected R, G, and B OLED elements. The highest occupied and the lowest unoccupied molecular orbital energies are taken from the literature.^{5,13} The 20 Ω/sq indium tin oxide (ITO) precoated

glass substrates were degreased in detergent solution and cleaned by solvents, followed by 10 min exposure to UV/ozone prior to transfer into a high vacuum ($\sim 10^{-7}$ Torr) deposition chamber. Then the B, G, and R OLEDs were sequentially deposited by thermal evaporation without breaking vacuum. A 10-nm-thick BPhen layer doped with Li in a 1:1 molar ratio combined with a 10-nm-thick layer of MoO₃ served as the CGLs between elements. The transmittance of

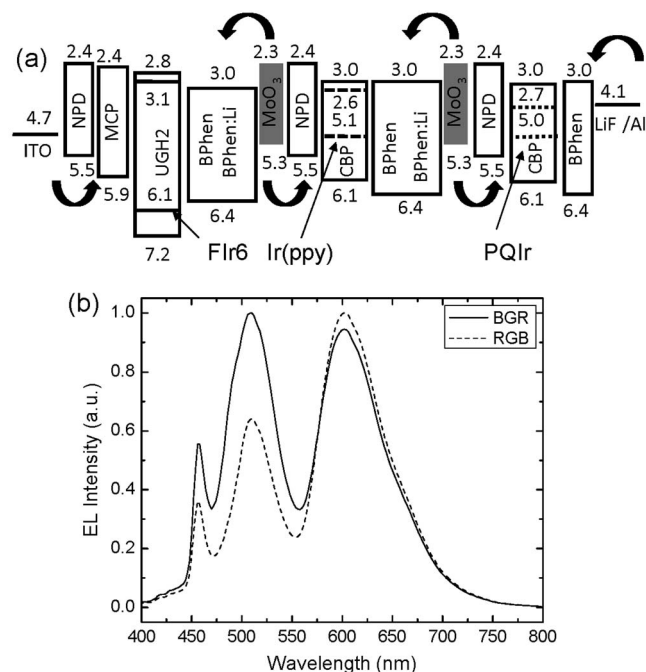


FIG. 1. (a) Proposed energy-level diagram of the RGB SOLED. Numbers indicate the highest occupied molecular orbital (HOMO) and lowest unoccupied molecular orbital (LUMO) energies relative to vacuum (in eV). The HOMO and LUMO energies of Fir6, Ir(ppy)₃, and PQIr are (6.1 and 3.1 eV), (5.1 and 2.6 eV) and (5.0 and 2.7 eV), respectively. Arrows indicate carrier injection from electrodes and the MoO₃ charge-generation layer. (b) Spectrum of the optically optimized B-G-R (with R adjacent to the ITO anode) ordered device (solid line) and spectrum of the R-G-B ordered structure in (a) (dashed line).

^{a)}Electronic mail: stevefor@umich.edu.

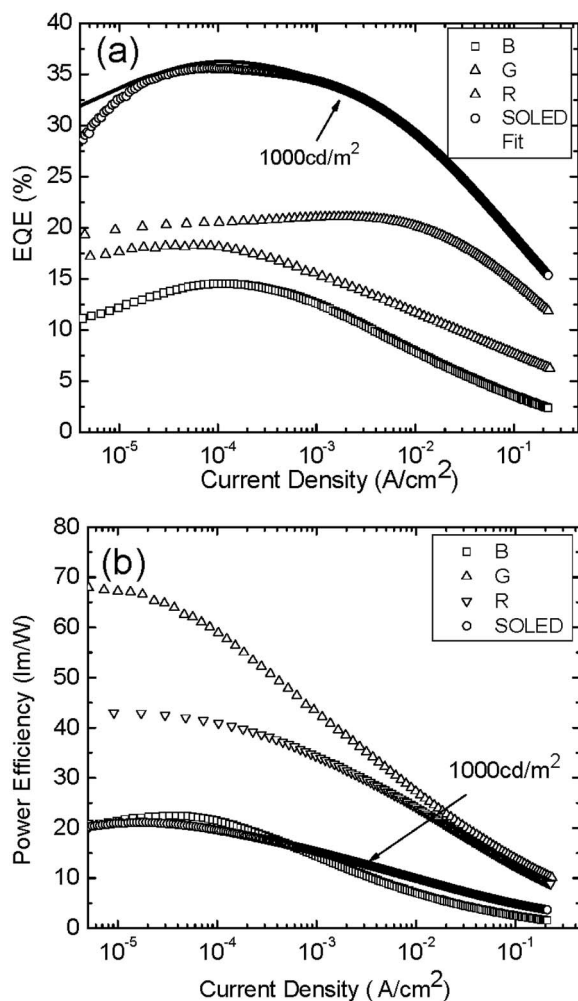


FIG. 2. (a) Total EQE of the RGB SOLED (open circles) along with that for the monochrome control devices. The solid line is a fit to the SOLED EQE, which is the weighted sum of the monochrome device efficiencies. (b) Total power efficiencies of the RGB SOLED and the control devices. Arrows indicate values at a brightness of 1000 cd/m².

the MoO₃ is 99.4% at a wavelength of 800 nm, decreasing to 96.1% at 450 nm. For each OLED element, a 40-nm-thick film of 4,4'-bis[*N*-(1-naphthyl)-*N*-phenyl-amino]-biphenyl (NPD) was used as the HTL, followed by a 25-nm-thick EML and a 50-nm-thick BPhen ETL. The undoped Bphen was used to prevent Li diffusion into the EML and to maintain charge balance at high bias.^{14,15}

To analyze the performance of the CGLs, three discrete monochrome R, G, and B control devices were simultaneously deposited with the SOLED. Each control has the same HTL and ETL and the same dopings, compositions, and thicknesses as the EMLs used in the SOLED. B, G, and R emissions originate from the phosphorescent dopants of bis-(4',6'-difluorophenylpyridinato) tetrakis(1-pyrazolyl)borate (FIr6), tris(phenylpyridine) iridium [Ir(ppy)₃], and Ir(III) bis-(2-phenylquinolyl-*N*,*C*2') acetylacetonate (PQIr), respectively. The optimized dopant/host combinations are FIr6:*p*-bis-(triphenylsilyl)benzene¹⁶ for B emission, Ir(ppy)₃:4,4'-*N,N'*-dicarbazole-biphenyl (CBP) for G, and PQIr:CBP for R. Doping concentrations are between 8 and 10 wt % for each cell. For the FIr6 device, a 10-nm-thick layer of *N,N'*-dicarbazolyl-3,5-benzene layer is inserted between the NPD and EML as an exciton blocking

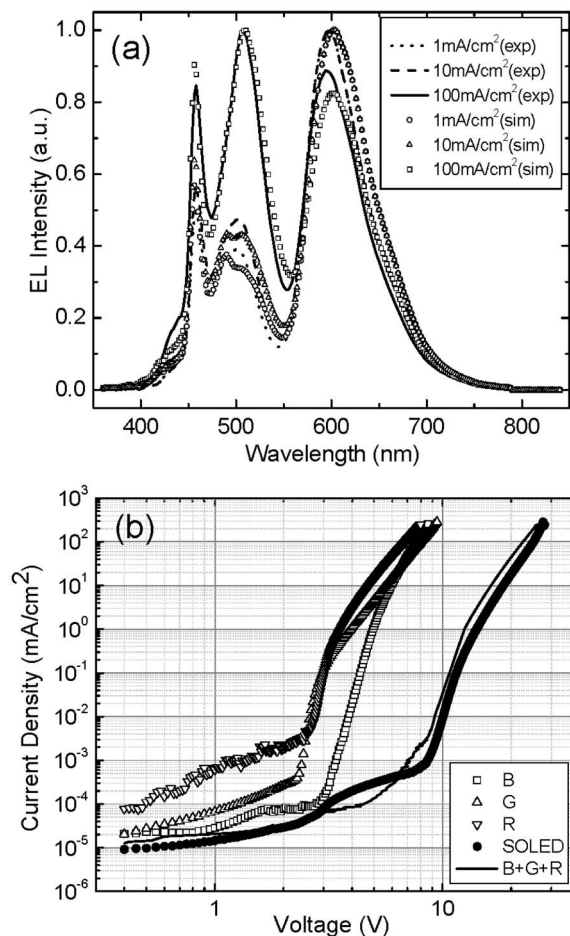


FIG. 3. (a) Measured and simulated spectra of the RGB SOLED at several current densities. Simulated spectra are based on cavity enhancement and extraction efficiencies by fitting the ratios of photons generated from the constituent R, G, and B elements. (b) Current-voltage (*J*-*V*) characteristics of the RGB SOLED and the monochrome control devices. The solid line is the sum of the currents of the three control devices, which in the absence of losses, would be equal to the RGB SOLED *J*-*V* characteristic.

layer. Finally, the cathode consisting of LiF (0.8 nm) and Al (120 nm) was deposited through a shadow mask with an array of 1.0 mm diameter openings.

For balanced emission from each OLED element, it is necessary to control the weak microcavity effects in the stacked device, which are calculated based on transfer matrix simulations. The refractive indices of organics, ITO, and MoO₃ employed in the simulation are 1.7, 1.9–0.036*j*, and 1.9–0.3*j*, respectively.⁷ By moving the three EMLs close to their optical antinodes, the order of B-G-R (with R adjacent to the ITO anode) leads to the optimal color balance, with Commission Internationale de L'Éclairage (CIE) coordinates (0.39, 0.42) and a color rendering index of CRI=79 [Fig. 1(b), solid line] at a current density of *J*=10 mA/cm², expected to result in a luminance >1000 cd/m². Two assumptions are made in this analysis: (i) each of the three dopant/host combinations has an internal quantum efficiency (IQE) equal to 100%, and the numbers of photons generated from each element are equal at a given current density, *J*; and (ii) the EQE of the stacked device follows the same roll-off behavior at high currents as each element, as shown in Fig. 2(a). The first assumption, as shown below, critically depends on the charge transport and injection properties of the CGLs for each element.

TABLE I. IQEs and the ratio of photons generated from the elements in the RGB SOLED.

	IQE			Photon ratio ^a		
	1 mA/cm ²	10 mA/cm ²	100 mA/cm ²	1 mA/cm ²	10 mA/cm ²	100 mA/cm ²
R (top)	0.69	0.67	0.48	1.00	1.00	1.00
G (middle)	0.84	0.65	0.42	0.45	0.64	2.22
B (top)	0.52	0.33	0.15	0.73	0.82	1.44

^aNumbers are normalized to the R element intensity.

The experimental spectra of this optically optimized RGB SOLED show distinct differences from calculation, with the PQIr peak intensity four to five times stronger than that of Fir6. This indicates that in addition to optical effects, the injection efficiency of charges from the CGL indeed plays a significant role in determining the output spectrum. We find that injection from ITO is more efficient than from MoO₃ used in the stacking configuration in Fig. 1(a). The optically optimized spectrum of this structure is shown in Fig. 1(b) as a dashed line.

The EQE and power efficiency of the RGB SOLED in Fig. 1(a) and the monochrome OLED control devices, measured in an integrating sphere, are shown in Fig. 2. B, G, and R controls exhibit EQE peaks at $(13.9 \pm 1.0)\%$, $(17.5 \pm 1.0)\%$, and $(20.1 \pm 1.0)\%$, respectively, typical for OLEDs based on this set of phosphor dopants and hosts.⁵ The total EQE and power efficiencies for the RGB SOLED peak at $\eta_{\text{ext}} = (36 \pm 2)\%$ at a current density of $J = 82 \mu\text{A}/\text{cm}^2$ and $\eta_p = 21 \pm 1 \text{ lm}/\text{W}$ at $J = 17 \mu\text{A}/\text{cm}^2$, respectively. These values roll off to $(32 \pm 2)\%$ and $13 \pm 1 \text{ lm}/\text{W}$ at $1000 \text{ cd}/\text{m}^2$ corresponding to $J = 2 \text{ mA}/\text{cm}^2$. The maximum EQE of the RGB SOLED is approximately the sum of the EQEs of the three individual elements over a wide range of current densities, indicating that the losses at the transparent CGL are minimal. A fit of SOLED EQE is shown by the solid line, yielding an emission intensity ratio 0.7:0.5:1 in the B, G, and R elements. This dependence of exciton formation on position in the stack is attributed to the different injection efficiencies of the CGLs and the ITO anode.

Figure 3(a) shows the experimental and simulated electrophosphorescence spectra for the RGB SOLED at several current densities. The Commission Internationale d'Eclairage (CIE) coordinates and color rendering index (CRI) values are (0.45, 0.36) and 63 at $J = 2 \text{ mA}/\text{cm}^2$ corresponding to $1000 \text{ cd}/\text{m}^2$ and (0.36, 0.37) and 78 at $J = 100 \text{ mA}/\text{cm}^2$. From the simulations, we determine the fraction of photons generated from each cell, with values listed in Table I. Note that NPD emission was observed to increase in intensity with J . Due to the relatively inefficient electron injection from MoO₃ compared to that of the Al cathode, electrons concentrate at the MoO₃/NPD interface, leading to some exciton formation on the NPD. To test this hypothesis, a two-color RG SOLED was grown, one with a 50-nm-thick BPhen layer adjacent to the CGL and the other with only a 30-nm-thick BPhen layer. No NPD emission is observed in the first case, nor for the R and G control devices, while a strong NPD signal is observed for the structure with thinner Bphen.

In Fig. 3(b) we show the current density versus voltage characteristics of the SOLED and the R, G, and B control devices. The excess drive voltage on the SOLED compared

with the sum of that on all three control devices (solid line) is due to energy barriers at the CGL. It accounts for a concomitant reduction of $(10.3 \pm 0.7)\%$ in power efficiency.

Table I provides the IQEs and the fraction of photons generated from the three stacked elements. As current density increases, we observe an increase in exciton formation on the B and G elements with respect to that of the R element. This indicates a current dependent electron and hole injection efficiency from the CGLs.

In summary, we have demonstrated an all-phosphorescent RGB SOLED using a compound MoO₃/Li:BPhen transparent CGL. White emission and SOLED efficiency were optimized by making a tradeoff between the color emissive element ordering to achieve efficient charge injection and a maximum outcoupling efficiency at a high CRI. The device reaches a maximum total EQE and power efficiency of $\eta_{\text{ext}} = (36 \pm 2)\%$ and $\eta_p = 21 \pm 1 \text{ lm}/\text{W}$, respectively. These results demonstrate that electrophosphorescent RGB SOLEDs represent a promising architecture in achieving high brightness and efficiency for indoor lighting.

The authors thank the U.S. Department of Energy and Universal Display Corporation for partial financial support.

- ¹B. W. D'Andrade and S. R. Forrest, *Adv. Mater. (Weinheim, Ger.)* **16**, 1585 (2004).
- ²J. H. Jou, M. C. Sun, H. H. Chou, and C. H. Li, *Appl. Phys. Lett.* **88**, 141101 (2006).
- ³B. W. D'Andrade, R. J. Holmes, and S. R. Forrest, *Adv. Mater. (Weinheim, Ger.)* **16**, 624 (2004).
- ⁴J. H. Seo, I. H. Park, G. Y. Kim, K. H. Lee, M. K. Kin, S. S. Yoon, and Y. K. Kim, *Appl. Phys. Lett.* **92**, 183303 (2008).
- ⁵Y. Sun and S. R. Forrest, *Appl. Phys. Lett.* **91**, 263503 (2007).
- ⁶H. Kanno, N. C. Giebink, Y. Sun, and S. R. Forrest, *Appl. Phys. Lett.* **89**, 023503 (2006).
- ⁷H. Kanno, R. J. Holmes, Y. Sun, S. Kena-Cohen, and S. R. Forrest, *Adv. Mater. (Weinheim, Ger.)* **18**, 339 (2006).
- ⁸Z. Shen, P. E. Burrows, V. Bulovic, S. R. Forrest, and M. E. Thompson, *Science* **276**, 2009 (1997).
- ⁹J. Drechsel, M. Pfeiffer, X. Zhou, A. Nollau, and K. Leo, *Synth. Met.* **127**, 201 (2002).
- ¹⁰X. D. Gao, J. Zhou, Z. T. Xie, B. F. Ding, Y. C. Qian, X. M. Ding, and X. Y. Hou, *Appl. Phys. Lett.* **93**, 083304 (2008).
- ¹¹C. W. Law, K. M. Lau, M. K. Fung, M. Y. Chan, F. L. Wong, C. S. Lee, and S. T. Lee, *Appl. Phys. Lett.* **89**, 133511 (2006).
- ¹²T. W. Lee, T. Noh, B. K. Choi, M. S. Kim, and D. W. Shin, *Appl. Phys. Lett.* **92**, 043301 (2008).
- ¹³H. J. Bolink, E. Coronado, D. Repetto, M. Sessolo, E. M. Barea, J. Bisquert, G. Garcia-Belmonte, J. Prochazka, and M. L. Kavan, *Adv. Funct. Mater.* **18**, 145 (2008).
- ¹⁴G. Parthasarathy, C. Shen, A. Kahn, and S. R. Forrest, *J. Appl. Phys.* **89**, 4986 (2001).
- ¹⁵N. C. Giebink and S. R. Forrest, *Phys. Rev. B* **77**, 235215 (2008).
- ¹⁶R. J. Holmes, B. W. D'Andrade, S. R. Forrest, X. Ren, J. Li, and M. E. Thompson, *Appl. Phys. Lett.* **83**, 3818 (2003).